Morphogenic Effects of Ezrin Require a Phosphorylation-induced Transition from Oligomers to Monomers at the Plasma Membrane

Alexis Gautreau, Daniel Louvard, and Monique Arpin

Laboratoire de Morphogénèse et Signalisation Cellulaires, UMR 144 CNRS/Institut Curie, 75248 Paris Cedex 05, France

Abstract. ERM (ezrin, radixin, moesin) proteins act as linkers between the plasma membrane and the actin cytoskeleton. An interaction between their NH_2- and COOH-terminal domains occurs intramolecularly in closed monomers and intermolecularly in head-to-tail oligomers. In vitro, phosphorylation of a conserved threonine residue (T567 in ezrin) in the COOH-terminal domain of ERM proteins disrupts this interaction. Here, we have analyzed the role of this phosphorylation event in vivo, by deriving stable clones producing wild-type, T567A, and T567D ezrin from LLC-PK1 epithelial cells. We found that T567A ezrin was poorly associated with the cytoskeleton, but was able to form oligomers. In contrast, T567D ezrin was associated with the cytoskeleton, but its distribution was shifted from oligomers to monomers at the membrane. Moreover, production of T567D ezrin induced the formation of lamellipodia, membrane ruffles, and tufts of microvilli. Both T567A and T567D ezrin affected the development of multicellular epithelial structures. Collectively, these results suggest that phosphorylation of ERM proteins on this conserved threonine regulates the transition from membrane-bound oligomers to active monomers, which induce and are part of actin-rich membrane projections.

Key words: ERM • head-to-tail interaction • conformation • actin • cytoskeleton

Introduction

ERM (ezrin, radixin, moesin)[1] proteins act as linkers between the plasma membrane and the actin cytoskeleton. Inactivation studies indicated that these proteins play a role in the formation of microvilli, cell–cell junctions, and membrane ruffles, and also regulate substrate adhesion and motility (Takeuchi et al., 1994; Crepaldi et al., 1997; Lamb et al., 1997). Regulation of ERM linker function is thought to occur through conformational changes (Bretscher, 1999).

ERM proteins possess two conserved domains. The NH_2-terminal domain is responsible for membrane targeting, whereas the COOH-terminal domain contains an F-actin binding site (Algrain et al., 1993; Turunen et al., 1994). These two domains interact strongly with each other, and have been termed N- and C-ERMADs, standing for ERM association domain (Gary and Bretscher, 1995; Magendantz et al., 1995). In ezrin, N-ERMAD has been mapped to the first 296 amino acids and C-ERMAD to the last 107 amino acids. Because of the intramolecular N/C-ERMAD interaction, most ERM proteins are in a cytosolic dormant form, in which binding sites for membrane components and F-actin are masked. In the NH_2-terminal domain, cryptic binding sites have been identified for Rho-GDI and EBP-50 proteins (Reczek et al., 1997; Takahashi et al., 1997; Reczek and Bretscher, 1998). Recently, the crystal structure of the moesin N-ERMAD bound to the C-ERMAD revealed a globular conformation for the N-ERMAD domain and an extended conformation for the C-ERMAD, which mutually mask binding sites (Pearson et al., 2000).

Intermolecular N/C-ERMAD interactions also form ERM oligomers. In purified placental microvilli, ezrin dimers, trimers, tetramers, and higher order oligomers were identified, suggesting a head-to-tail assembly (Berryman et al., 1995). These oligomers are proposed to be associated with the cytoskeleton and to be involved in microvillar morphogenesis. However, soluble ezrin dimers were also detected (Bretscher et al., 1995). Oligomerization is not specific to ezrin, since mixed oligomers containing different ERM members were observed (Gary and Bretscher, 1993; Andréoli et al., 1994). To engage ERMADs in intermolecular interactions, cytosolic dormant monomers are thought to be subjected to a gross conformational change. This phenomenon does not occur spontaneously

Address correspondence to Monique Arpin, Laboratoire de Morphogénèse et Signalisation Cellulaires, UMR 144 CNRS/Institut Curie, 26 rue d'Ulm, 75248 Paris Cedex 05, France. Tel.: 33 1 42 34 63 72. Fax: 33 1 42 34 63 77. E-mail: marpin@curie.fr

[1]*Abbreviations used in this paper:* C-ERMAD, COOH-terminal ERM association domain; ERM, ezrin, radixin, moesin; N-ERMAD, NH_2-terminal ERM association domain; wt, wild-type.

in vitro with purified ezrin, and probably requires an activation step (Bretscher et al., 1995).

Phosphorylation has been proposed to regulate ERM activation, since phosphorylation of ERM proteins correlates with their cytoskeletal association (Chen et al., 1994; Kondo et al., 1998; Simons et al., 1998). Ezrin is phosphorylated on tyrosine residues upon growth factor stimulation (Gould et al., 1989; Fazioli et al., 1993; Crepaldi et al., 1997). In response to EGF, ezrin phosphorylation on tyrosines 145 and 353 is concomitant with an increase in dimer formation, suggesting a causal relationship between phosphorylation and oligomerization (Krieg and Hunter, 1992; Berryman et al., 1995). However, mutations of these tyrosines into phenylalanines does not alter ezrin localization in microvilli, and production of this mutated ezrin does not affect cell morphology (Crepaldi et al., 1997). Rather than controlling its cytoskeletal association, tyrosine phosphorylation of ezrin appears to transduce signals. For example, phosphorylation of tyrosine 353 was found to signal cell survival during epithelial differentiation (Gautreau et al., 1999).

Another phosphorylation site is a better candidate to activate ERM cytoskeletal linkage. A phosphothreonine residue, originally identified in moesin (Nakamura et al., 1995), is localized in a conserved COOH-terminal region of ERM proteins (T567 in ezrin, T564 in radixin, and T558 in moesin). Using phosphospecific antibodies, this phosphorylated residue was detected in ezrin, radixin, and moesin from a variety of cells and tissues, and phosphorylated ERM proteins were shown to be present in actin-rich membrane structures (Nakamura et al., 1996; Matsui et al., 1998; Oshiro et al., 1998; Hayashi et al., 1999). Two kinases, protein kinase C-theta (PKC-θ) and Rho-kinase, and two phosphatases, myosin phosphatase and type 2C protein phosphatase (PP2C), were found in different systems to regulate the phosphorylation status of this conserved threonine in ERM proteins (Fukata et al., 1998; Matsui et al., 1998; Pietromonaco et al., 1998; Hishiya et al., 1999).

The primary consequence of this phosphorylation event is to impair N/C-ERMAD interaction. In an overlay assay, phosphorylation of T564 in radixin COOH-terminal domain impairs its association with the NH_2-terminal domain (Matsui et al., 1998). Similarly, the T558D mutation of moesin, which mimics the phosphorylated state, was shown to affect the N/C-ERMAD interaction (Huang et al., 1999). From the crystal structure, it appears that the phosphorylation of moesin T558 weakens the N/C-ERMAD interaction due to both electrostatic and steric effects (Pearson et al., 2000). The phosphorylation of an isolated COOH-terminal fragment of ERM proteins does not affect its association with F-actin (Matsui et al., 1998; Huang et al., 1999). However, in full-length ERM proteins, phosphorylation of this conserved threonine is required to bind to F-actin (Simons et al., 1998; Hishiya et al., 1999; Nakamura et al., 1999). These results suggest that phosphorylation of this residue activates ERM cytoskeletal association by unmasking the cryptic F-actin binding site. Furthermore, expression of T into D mutant forms of ezrin or moesin potentiates the formation of microvilli-like dorsal projections by growth factors (Oshiro et al., 1998; Yonemura et al., 1999), whereas transfection of the nonphosphorylatable T558A moesin inhibits RhoA-induced formation of these structures (Oshiro et al., 1998; Shaw et al., 1998).

Although phosphorylation of this conserved threonine residue regulates the activation of ERM cytoskeletal linkers, the mechanism of this regulation is still poorly understood. By disrupting N/C-ERMAD interaction, this phosphorylation event could trigger the opening of dormant monomers, could impair oligomerization, or both. To clarify the mechanism of ERM conformational regulation, we analyzed the role of ezrin T567 phosphorylation in LLC-PK1 epithelial cells. We found that T567D ezrin exhibited a drastic reduction in the amount of oligomers at the plasma membrane. Monomeric T567D ezrin was associated with the actin cytoskeleton and induced actin-rich membrane projections. Production of T567D ezrin strongly affected epithelial morphology and differentiation. In contrast, T567A ezrin exhibited a level of membrane oligomers similar to wild-type (wt), but was poorly associated with the actin cytoskeleton. These results suggest that phosphorylation of this conserved threonine regulates a membrane-specific transition from oligomers to monomers, which are active plasma membrane–actin cytoskeleton linkers.

Materials and Methods

Cells and Recombinant Proteins

LLC-PK1 cells (CCL 101; American Type Culture Collection) were cultured in DME containing 10% FCS and maintained at 37°C in 10% CO_2. Recombinant NH_2-terminal fragment 1–309 of ezrin was produced and purified as a GST fusion as previously described (Gautreau et al., 1999). GST moiety was cleaved off by thrombin digestion. Recombinant NH_2-terminal fragment was biotinylated with NHS-LC-biotin (Pierce Chemical Co.) according to the manufacturer's instructions.

cDNA Constructs and Transfection

To substitute T567 with A567 or D567, PCR reactions were performed with oligonucleotides in which the codon ACG was replaced by GCG or GAC, respectively. The amplified fragments were subcloned into the pCB6 vector containing VSV G-tagged ezrin cDNA (Algrain et al., 1993). Myc-tagged ezrin was cloned in pCDNA 3.1 vector (Invitrogen). All PCR fragments were verified by sequencing.

For transfection, trypsinized cells were resuspended at a concentration of 2.5×10^7 cells/ml in 15 mM Hepes, pH 7.4, buffered medium. 200 μl of cell suspension was added to 50 μl of a solution containing 210 mM NaCl, 5 μg of plasmid DNA, and 30 μg of salmon sperm DNA carrier (Sigma-Aldrich). LLC-PK1 cells were electroporated with a BioRad Gene Pulser at 950 μF and 240 V using 4-mm width cuvettes. Transiently transfected cells were analyzed after 48 h of cDNA expression. Clones producing T567A and T567D ezrin were established as previously described, and were compared with the previously obtained clones transfected with the empty plasmid or producing wt ezrin (Crepaldi et al., 1997).

Cytosol/Membrane Fractionation and Gel Filtration Analysis

Cells from a confluent 10-cm dish (for standard immunoprecipitation), or from ten confluent 10-cm dishes (for the Coomassie blue-stained immunoprecipitation experiment or gel filtration analysis), were rinsed once with cold PBS, once with cold cyt buffer (10 mM Hepes, 1 mM EDTA, 150 mM NaCl, pH 7.4), and scraped off with a rubber policeman in 1 ml of cold cyt buffer supplemented with protease inhibitors (200 μg/ml pefabloc, 15 μg/ml benzamidine, 1 μg/ml pepstatin, 1 μg/ml antipain). Cells in suspension were mechanically disrupted by 10 strokes of a cell cracker. Debris and nuclei were pelleted by a 10-min centrifugation at 600 *g* at 4°C. The supernatant was then subjected to a 20-min centrifugation at 100,000 *g* using a

TLA-120.2 rotor in an optima TLX ultracentrifuge (Beckman Coulter). This ultracentrifugation pellets crude membranes, whereas the supernatant is the cytosolic fraction.

For gel filtration analysis, membrane pellets were further extracted by a 15-min incubation in 200 μl of mbn buffer (10 mM Hepes, 1 mM EDTA, 600 mM KCl, 1% Triton X-100, pH 7.4) supplemented with protease inhibitors, and then ultracentrifuged again. 200 μl of cytosol or membrane extracts were loaded onto a superose-6 HR10/30 gel filtration column (Amersham Pharmacia Biotech), preequilibrated with cyt or mbn buffer respectively, and run at a flow rate of 300 μl/min. 250 μl fractions were collected. The column was calibrated with thyroglobulin, ferritin, aldolase, and BSA (Sigma-Aldrich) as standards. Thyroglobulin (Stokes radius of 85 Å), ferritin (61 Å), aldolase (48 Å), and BSA (35.5 Å) peaked at fractions 24, 32, 41, and 43, respectively. Void volume of the column emerged in fraction 3.

When endogenous ERM phosphorylation was examined, cyt and mbn buffers were also supplemented with 2 mM of sodium pyrophosphate and 1 μM of calyculinA (Upstate Biotechnology). When indicated, LLC-PK1 cells were pretreated for 10 min at 37°C with 300 nM of calyculinA. For oligomer and monomer samples of Fig. 2, 150 μl of fractions 24–27 and 150 μl of fractions 35–38 were pooled and precipitated by 2 min at 100°C, followed by 10 min at 4°C. For efficient precipitation of the oligomeric fraction, 15 μg of BSA was added before boiling, because this fraction contained a low amount of proteins. The precipitates were pelleted by a 10-min centrifugation at 20,000 *g* at 4°C, and resuspended in SDS-loading buffer.

Immunoprecipitations

Cytosol or total extracts were adjusted to 1 ml of RIPA buffer (50 mM Hepes, 10 mM EDTA, 150 mM NaCl, 1% NP-40, 0.5% sodium deoxycholate, 0.1% SDS, pH 7.4). Membrane pellets were resuspended in RIPA buffer. RIPA extracts were supplemented with protease inhibitors. For the experiment in which denatured extracts are used, cells were lysed in 1 ml of 50 mM Hepes, 10 mM EDTA, 150 mM NaCl, 1% NP-40, pH 7.4, buffer. The extracts were adjusted to 1% SDS and boiled for 2 min. Denatured extracts were then put on ice for 10 min and diluted to 10 ml with a cold buffer reconstituting RIPA composition.

Extracts were clarified by 10 min centrifugation at 20,000 *g* at 4°C, and incubated with 10 μl of protein A–Sepharose fast-flow beads (Amersham Pharmacia Biotech) and 5 μg of affinity-purified ezrin or VSV G rabbit polyclonal antibodies for 2 h (1 ml vol) or overnight (10 ml vol). Beads were washed five times with 1 ml of RIPA buffer, and boiled 2 min in SDS loading buffer.

Overlay and Western Blotting

All blots were performed on nitrocellulose membranes (Protran Hybond). P5D4 anti-VSV G mAb, 9E10 anti-myc mAb, phosphospecific 297S mAb (a kind gift of Dr. S. Tsukita, Kyoto University, Japan), anti-moesin affinity-purified mouse polyclonal antibodies, anti-radixin affinity-purified guinea pig polyclonal antibodies (both kind gifts of Dr. P. Mangeat, University of Montpellier, France), anti-ezrin affinity-purified rabbit polyclonal antibodies (Algrain et al., 1993), or biotinylated NH_2-terminal domain of ezrin were used as primary reagents, and alkaline phosphatase-coupled immunoglobulins or streptavidin, as secondary reagents (Promega). Blots were developed with nitroblue tetrazolium/5-bromo, 4-chloro, 3-indolyl phosphate as substrates (Promega). The intensities of bands were quantitated by scanning densitometry on a Bio-Profil station (Vilbert-Lourmat).

Immunofluorescence and Microscopy

Cell morphology was examined by phase-contrast optics or by Nomarski optics on a Leica microscope. For scanning EM, cells grown at confluence on 10-mm 0.2 μm anopore membrane filters (Nunc) were dehydrated in graded ethanol baths, dried by the critical point method using liquid CO_2, coated with gold palladium, and observed with a JEOL microscope (JSM 840A).

Immunolocalization of exogenous ezrin was achieved with VSV G affinity-purified polyclonal antibodies at 10 μg/ml and Cy-2–conjugated goat anti–rabbit secondary antibodies (Jackson ImmunoResearch Laboratories) on fixed and permeabilized cells using the paraformaldehyde/Triton X-100 protocol previously described (Crepaldi et al., 1997). Samples were examined with a Leica confocal laser-scanning microscope, using the same settings for all acquisitions.

Analysis of Cytoskeletal Fraction

Confluent cultures from 6 well plates were rinsed quickly with PBS at room temperature. The soluble fraction was extracted by a 1-min incubation with 500 μl of a Triton X-100 buffer that preserves cytoskeleton-associated material (csk buffer: 50 mM MES, 3 mM EGTA, 5 mM $MgCl_2$, 0.5% Triton X-100, pH 6.4) at room temperature. For immunofluorescence analysis, the insoluble material was immediately fixed in 3% paraformaldehyde. We verified that actin and microtubule cytoskeletons were not affected by this treatment. For immunoblot analysis, the insoluble material was quickly rinsed with 500 μl of csk buffer, and further extracted by a 1-min incubation with 500 μl of ice-cold RIPA buffer. When endogenous ERM phosphorylation was examined, csk and RIPA buffers were also supplemented with 2 mM of sodium pyrophosphate and 1 μM of calyculinA.

Development of Multicellular Epithelial Structures

For the suspension cyst assay, 25-ml siliconized erlenmeyers containing 5 ml of a cell suspension at 10^6 cells/ml in 15 mM Hepes, pH 7.4, buffered medium were rocked in a shaking incubator at 75 rpm (ROSI 1000; Thermolyne). Cultures were analyzed after 48 h. For the tubulogenesis assay, cells were seeded in a collagen type I gel, as previously described (Gautreau et al., 1999). 1-wk cultures, in DMEM containing 10% FCS and 100 U/ml of HGF, were examined. Importantly, in these two assays, all clones isolated in each category behaved similarly.

Results

T567D Ezrin Exhibits a Low Amount of Oligomers at the Membrane

We chose to study ezrin function in LLC-PK1 epithelial cells, which are derived from kidney proximal tubule. This cell line retains many features of proximal tubule cells, since it harbors numerous microvilli at its apical surface, and coexpresses ERM proteins (Berryman et al., 1993). To analyze the role of ezrin T567 phosphorylation, cDNAs encoding a nonphosphorylatable variant, T567A ezrin, and a pseudophosphorylated variant, T567D ezrin, were expressed in LLC-PK1 cells. We derived stably transfected clonal cell lines producing wt, T567A, or T567D ezrin, called E, A, or D cells, respectively, and we compared them to control clones transfected with the empty plasmid, called P cells. The exogenous proteins were tagged at the COOH terminus with a VSV G epitope so they could be readily distinguished from the endogenous ezrin. The amount of exogenous ezrin relative to endogenous ezrin was estimated to be about tenfold higher in the isolated clones, by immunoblotting serially diluted extracts with the antiezrin antibody (data not shown).

To assess if the T567D mutation of ezrin impairs the N/C-ERMAD interaction, we analyzed wt, T567A, and T567D ezrin for their binding to biotinylated N-ERMAD in a blot overlay assay. We immunoprecipitated endogenous ezrin or VSV G-tagged ezrin variants from denatured lysates derived from P, E, A, and D cells. This allowed the isolation of ezrin without associated proteins. An equivalent amount of ezrin and VSV G-tagged wt, T567A, and T567D ezrin was immunoprecipitated as revealed by ezrin immunoblotting (Fig. 1 A). The endogenous ezrin and VSV G-tagged wt ezrin bound strongly to the N-ERMAD, indicating that the VSV G tag has little influence, if any, on the N/C-ERMAD interaction. In contrast to wt and T567A ezrin, which bind efficiently to the ezrin N-ERMAD, the ability of T567D ezrin to interact with N-ERMAD was substantially diminished. This result

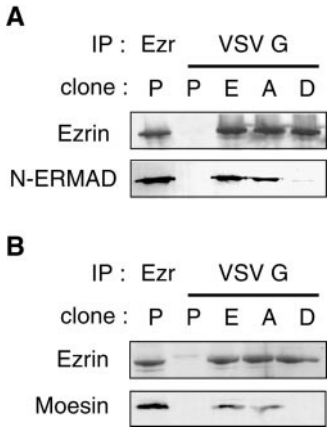

Figure 1. T567D ezrin has a reduced N-ERMAD binding activity in vitro, and does not oligomerize with moesin at the membrane in vivo. Throughout this study, clones producing VSV G-tagged wt ezrin, T567A ezrin, T567D ezrin (E, A, and D cells, respectively) or clones obtained after transfection of the empty plasmid (P cells) were compared. (A) Denatured extracts from P, E, A, and D clones were used to immunoprecipitate ezrin or VSV G-tagged wt, T567A, and T567D ezrin. The immunoprecipitates were probed with ezrin antibodies or with biotinylated ezrin N-ERMAD (1–309). (B) Ezrin from P, E, A, or D cell membrane extracts was immunoprecipitated with either anti-ezrin antibodies or anti-VSV G antibodies as indicated. After SDS-PAGE, the immunoprecipitates were stained by Coomassie blue to reveal ezrin (top), or immunoblotted with moesin-specific antibodies (bottom). Moesin associated with ezrin can be seen in the Coomassie blue–stained gel as a faint band just below the strong ezrin band.

suggests that the T567D mutation of ezrin mimics the phosphorylation of the C-ERMAD, at least in its disruptive effect on the N/C-ERMAD interaction (Matsui et al., 1998; Huang et al., 1999; Pearson et al., 2000).

In our current view of ERM activation, a discrepancy remains unresolved. On one hand, the active ERM protein, which is bound to the plasma membrane and the actin cytoskeleton, is expected to be oligomeric (Bretscher, 1999). On the other hand, an ERM protein requires the phosphorylation of this conserved threonine of the COOH-terminal domain to bind to F-actin (Nakamura et al., 1999). However, phosphorylation might disrupt the oligomeric form, through its impairment of intermolecular N/C-ERMAD interaction. To examine ERM oligomerization, we looked at whether the ezrin variants were associated with endogenous moesin. We immunoprecipitated ezrin from the membrane pool to enrich for the active form. The immunoprecipitates were either stained with Coomassie blue or immunoblotted with moesin-specific antibodies (Fig. 1 B). A high amount of ezrin was precipitated with anti-ezrin or anti-VSV G antibodies, as seen by Coomassie blue staining. Moesin coprecipitated with endogenous ezrin, exogenous wt, and T567A ezrin, but not with T567D ezrin. This lack of hetero-oligomerization of T567D ezrin with moesin in the membrane fraction suggests that the T567D mutation of ezrin impairs intermolecular N/C-ERMAD interactions. An association with radixin could not be determined, because the immunoprecipitated ezrin gave a high background at the position of radixin, which migrates only slightly faster than ezrin in SDS-PAGE.

To examine directly the oligomeric status of T567 mutant forms of ezrin, we used a procedure that resolves ezrin oligomers from monomers (Berryman et al., 1995). First, we examined the distribution of endogenous ezrin in P cells. Ninefold less ezrin is found in the membrane fraction compared with the cytosolic fraction (Table I). Membrane and cytosolic extracts from the P cells were applied to a superose-6 gel filtration column. Oligomers were detected in the cytosol, as well as in the membrane fraction (Fig. 2 A). Even if most oligomers were cytosolic (Table I), the relative level of oligomers over the total ezrin at the membrane was about twofold that in the cytosol (28% of oligomers at the membrane vs. 15% of oligomers in the cytosol). Then, we examined the oligomer profile for the ezrin variants (Fig. 2 A). In the membrane extracts, ezrin oligomers were observed with wt and T567A ezrin. However, consistent with its lack of association with moesin, T567D ezrin from the membrane fraction was eluted essentially as monomers, with only a trace amount of oligomers. Interestingly, in the cytosol, no differences between ezrin variants were noted. Thus, T567D ezrin exhibited a strong reduction in the amount of oligomers exclusively at the membrane.

Table I. Quantification of the Ezrin Content in the Different Pools

	Cell debris	Cytosol	Membrane	Membrane ins.
	%	%	%	%
Total	8.8	81.9	9.3	0.057
Monomers	–	69.6	6.7	–
Oligomers	–	12.3	2.6	–

The amount of ezrin was quantified by Western blotting serially diluted fractions. Cells were mechanically cracked. Cell debris refers to the 600-*g* pellet that also contained nuclei and unbroken cells. The supernatant was then separated by a 100,000-*g* centrifugation into a cytosolic supernatant and a membrane-containing pellet. The pellet was extracted with a high salt Triton X-100 buffer. Membrane ins. refers to the 100,000-*g* pellet after its extraction (see Materials and Methods). Monomers and oligomers were separated by gel filtration chromatography and the corresponding fractions were pooled. These data are the means of two independent fractionations.

Phosphorylated ERM Proteins Are Preferentially Monomeric at the Membrane

The analysis of T567D ezrin indicated that the effect of phosphorylation occurs at the membrane. To get insight into the distribution of phosphorylated endogenous ERM proteins from LLC-PK1 cells, we used 297S, an mAb recognizing this conserved phosphorylated threonine of ERM COOH-terminal domain (Matsui et al., 1998). We examined the distribution of phosphorylated ERM proteins between the membrane and the cytosol. When a similar amount of ERM proteins from total, cytosol, and membrane fractions was blotted with 297S, phosphorylated ERM proteins appeared highly enriched in the membrane fraction (Fig. 2 B). This result is consistent with the membrane-dependent effect of the ezrin T567D mutation.

Because the T567D mutation reduced the amount of ezrin oligomers at the membrane, we hypothesized that the phosphorylation of this threonine dissociates ezrin oligomers into monomers. If this hypothesis is correct, monomers should be more phosphorylated than oligomers. Our initial attempts to determine which of the monomers or the oligomers were preferentially phosphorylated failed because of dephosphorylation during the gel filtration procedure. To overcome this problem, we pretreated LLC-PK1 cells with calyculinA, a serine/threonine protein phosphatase inhibitor known to affect moesin

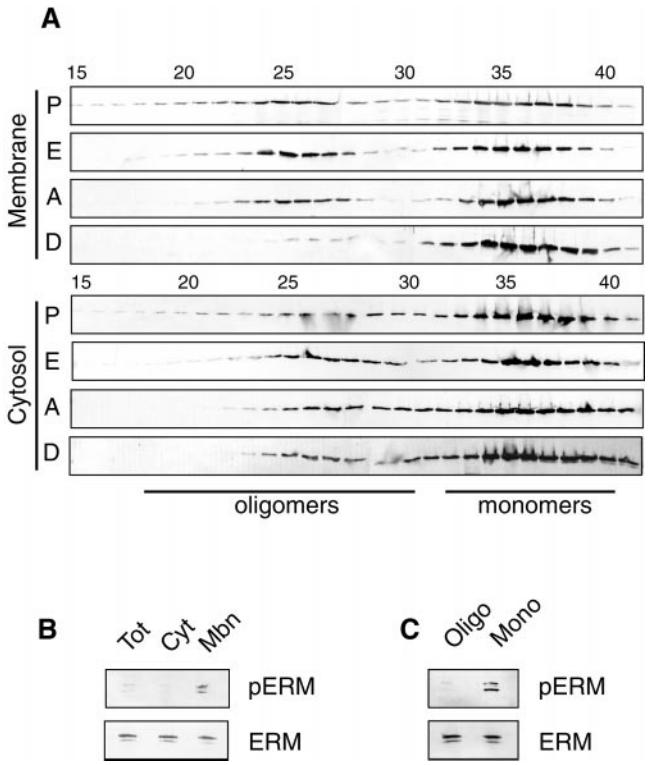

Figure 2. T567D ezrin and endogenous phosphorylated ERM proteins are preferentially monomeric at the plasma membrane. A, Membrane or cytosolic extracts from P, E, A, and D cells were resolved by gel filtration chromatography on a superose-6 column. Fractions 15–41 were analyzed by SDS-PAGE and immunoblotted with antiezrin antibodies (P) or anti-VSV G antibodies (E, A, and D). T567D ezrin exhibited a strongly reduced amount of oligomers at the membrane, but not in the cytosol. B, Total, cytosolic, and membrane extracts were immunoblotted with 297S mAb, recognizing all three ERM proteins when phosphorylated on this conserved threonine (pERM), or with a mixture of antibodies specific for ERM. Ezrin and radixin comigrated at ~80 kD, and moesin migrated at 75 kD. Phosphorylated ERM proteins were strongly enriched in the membrane fraction. C, LLC-PK1 cells were pretreated with calyculinA, a protein phosphatase inhibitor, and the membrane extract was resolved by gel filtration chromatography. Oligomeric and monomeric fractions were pooled, and immunoblotted as in B. Monomers were preferentially phosphorylated over oligomers.

phosphorylation (Nakamura et al., 1995). This treatment enhanced the phosphorylation signal and preserved it during gel filtration. Consistent with the preferential distribution of T567D ezrin in the monomeric fraction, ERM monomers were found to be preferentially phosphorylated over oligomers (Fig. 2 C).

Membrane/Cytosol Distribution of T567D Ezrin Is Regulated through its Functional C-ERMAD Domain

These results suggest that phosphorylation of ezrin occurs at the membrane, and dissociates oligomers, through an impairment of intermolecular N/C-ERMAD interaction at the membrane. However, we were intrigued by the fact that T567D ezrin was not defective in cytosolic oligomerization. This result is compatible with the hypothesis that the C-ERMAD of T567D ezrin is functional for oligomerization in the cytosol, but not at the membrane. To confirm in vivo that T567D ezrin has a functional C-ERMAD in the cytosol, we compared T567D ezrin to Δ29 ezrin, a form in which the 29 COOH-terminal amino acids were eliminated. Such a deletion completely abrogates C-ERMAD activity, i.e., N-ERMAD binding (Gary and Bretscher, 1995; data not shown). We devised a sensitive assay to study specifically ezrin homo-oligomerization. We transiently cotransfected LLC-PK1 cells with two ezrin cDNAs, one of them being tagged by the VSV G epitope, the other by the myc epitope, and examined the amount of ezrin–myc coprecipitating with ezrin–VSV G.

We analyzed the distribution of produced proteins between the membrane and cytosol pools (Fig. 3). Half of the transfected cell sample was analyzed directly (total), and the other half was separated in cytosolic and membrane fraction before analysis, so that the three pools were comparable. In total lysates, similar amounts of wt, T567A, T567D, and Δ29 ezrin were detected. In all transfections, a

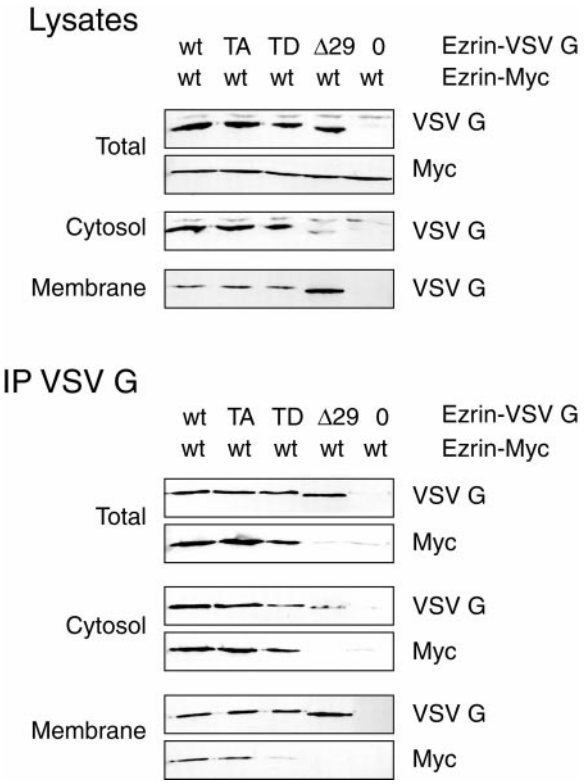

Figure 3. In the cytosol, T567D ezrin has a functional C-ERMAD. Various VSV G-tagged cDNAs, wt, T567A, and T567D ezrin, or an ezrin construct lacking a C-ERMAD due to the deletion of the 29 COOH-terminal amino acids (Δ29), were cotransfected with myc-tagged wt ezrin cDNA into LLC-PK1 cells to detect oligomerization. Total, cytosol, or membrane lysates (top) or VSV G immunoprecipitates of these lysates (bottom) were analyzed by immunoblotting with anti-VSV G or anti-Myc antibodies as indicated on the right of each panel. Δ29 ezrin was strongly enriched in the membrane fraction, and completely defective in oligomer formation. In contrast, T567D ezrin was correctly distributed between the cytosolic and the membrane fraction, and exhibited a strongly reduced amount of oligomers specifically at the membrane.

similar amount of ezrin–myc was produced. Analysis of cytosolic and membrane fractions revealed that wt, T567A, and T567D ezrin were similarly distributed between cytosol and membrane, most of ezrin being in the cytosol. In contrast, Δ29 ezrin was highly enriched in the membrane fraction. VSV G-tagged proteins were immunoprecipitated, and the immunoprecipitates were analyzed by immunoblotting with either anti-VSV G or antimyc antibodies. In total lysates, wt, T567A, and T567D ezrin oligomerized to roughly the same extent, whereas Δ29 ezrin was completely unable to form oligomers. T567A ezrin exhibited no difference with wt ezrin in its oligomerization ability in the cytosol and at the membrane. Consistent with gel filtration analysis, oligomers of T567D ezrin were present in the cytosol, but only as a trace amount at the membrane.

These data suggest that a functional C-ERMAD is needed both to mask membrane binding sites in the NH_2-terminal domain, and to form oligomers. T567D ezrin has a functional C-ERMAD in the cytosol, since T567D ezrin forms cytosolic oligomers and is correctly distributed between the cytosol and the membrane. However, upon membrane recruitment, the N/C-ERMAD interaction is abolished by the T567D mutation, and membrane oligomers of T567D ezrin are dissociated.

Dramatic Morphological Changes of LLC-PK1 Cells Producing T567D Ezrin

We asked whether there was a consequence of producing monomeric T567D ezrin on actin-rich membrane structures. We examined the morphology of LLC-PK1 clones producing wt, T567A, or T567D ezrin and the control clones transfected with the empty plasmid. E clones formed typical epithelial islets in sparse cell culture (Fig. 4 A), as did A and P clones (data not shown). These islets were composed of cells adhering to each other. The islet periphery was regular. In sharp contrast, all the D clones had an altered morphology. Some space between cells could be distinguished. The edges of D colonies were not smooth, but interrupted by wide lamellipodia. Those lamellipodia were sometimes at the tip of long extensions. By phase contrast, a refractile relief was also prominent at the position of the nucleus in most D cells. By scanning EM, this relief was shown to be due to extensive membrane ruffling (Fig. 4 B).

We observed confluent cultures of P, E, A, and D cells for optimal epithelial polarization and development of microvilli. Microvilli containing apical surface of these cells were analyzed by scanning EM. Production of wt or T567A ezrin did not alter microvillar density, length or organization, which were similar to those of control P cells (Fig. 5). In these confluent cultures, D cells formed a less organized layer of cells. The layer of flat cells was often interrupted by holes that exposed the filter surface, and some round cells attached above this flat cell layer were frequently observed. We verified that these round structures were indeed cells by fluorescent staining of nuclei (data not shown). Flat cells were covered with microvilli similar to controls, whereas round cells were covered with denser and longer microvilli. Occasionally, on the flat cell layer, microvilli developed aberrantly into tufts (Fig. 5). Such a tree-like organization of microvilli was never observed in P, E, or A cultures. In conclusion, production of monomeric T567D ezrin in LLC-PK1 cells induces numerous actin-rich membrane structures, such as lamellipodia, ruffles, and projections that are covered with microvilli.

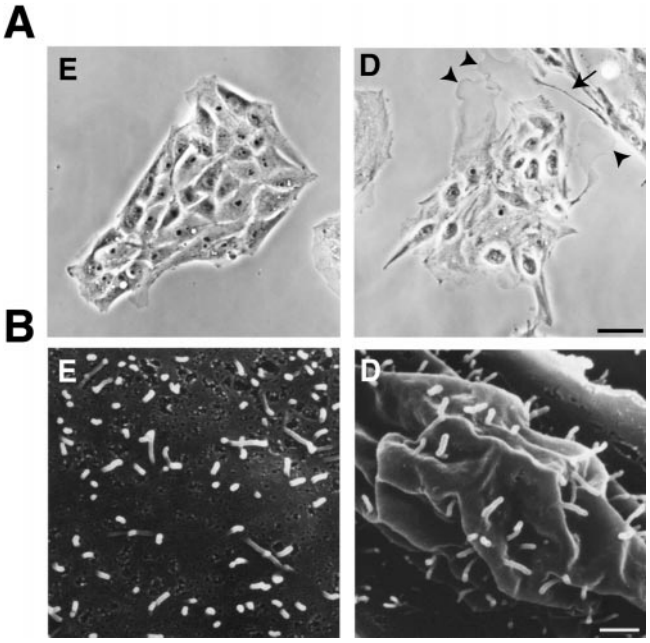

Figure 4. Morphology of LLC-PK1 cells producing T567D ezrin. (A) Clones were examined by phase-contrast optics. P, E, and A cells grew in typical LLC-PK1 islets (only the E control is presented). D colonies exhibited a number of morphological changes. In D colonies, cells were not always adherent to each other. The periphery of D colonies was irregular with wide lamellipodia (arrowheads). Those lamellipodia were occasionally formed at the extremity of long extensions (arrow). In most D cells, the membrane area around the nuclei was highly refractile. Bar, 25 μm. (B) Scanning EM examination of E and D cell morphology. Extensive membrane ruffling was observed in the cell central area, probably corresponding to the refractility observed by phase-contrast optics. Bars: (A) 25 μm; (B) 1 μm.

Ezrin Association with the Actin Cytoskeleton Requires Phosphorylation of T567

Because these ezrin variants displayed differential capacity to affect membrane morphogenesis, we compared their ability to associate with the actin cytoskeleton. Localization of exogenous ezrin by immunofluorescence was performed with anti-VSV G antibodies on confluent cultures of E, A, and D cells. Wt and T567A ezrin were detected in microvilli (Fig. 6 A), in a pattern similar to the one of endogenous ezrin in LLC-PK1 cells (data not shown). In the D cultures, T567D ezrin was found in microvilli of both flat and round cells and in ruffles. To evaluate whether these ezrin variants were associated with the actin cytoskeleton, we used an extraction procedure with a Triton X-100 buffer, which preserves the cytoskeleton and cytoskeleton-associated proteins. After extraction, wt ezrin and T567D ezrin were still detected in microvilli. In sharp contrast, T567A ezrin was almost completely extracted. Consistently, when Triton X-100 buffer–extracted

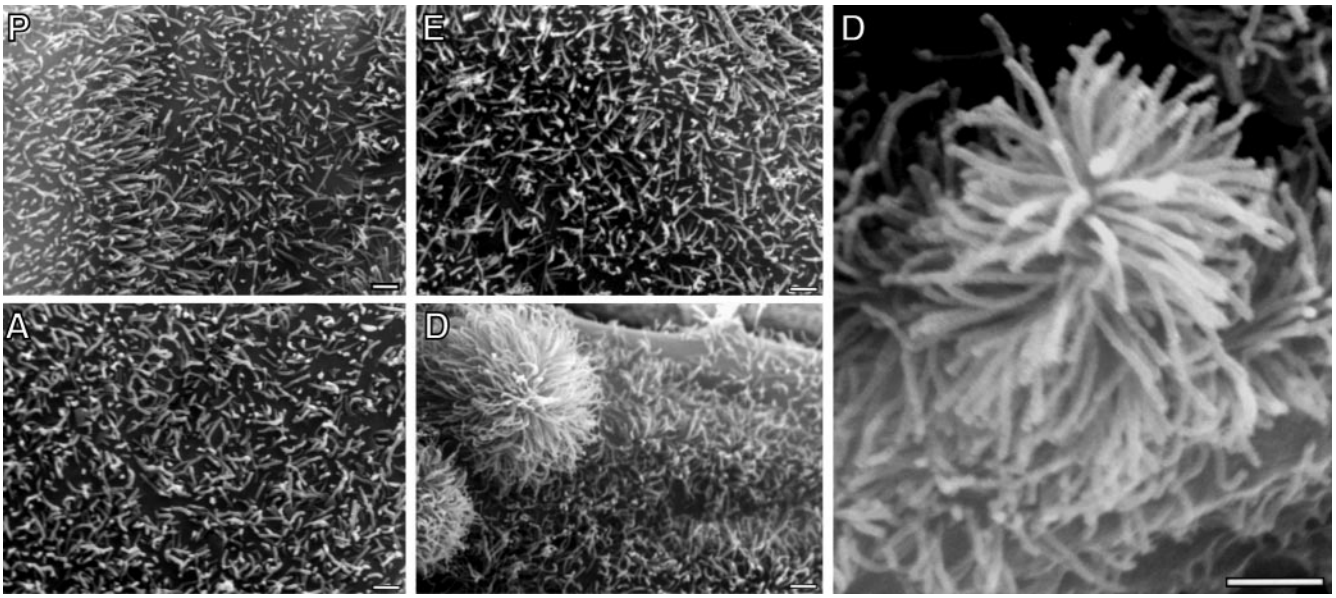

Figure 5. Scanning EM analysis of microvilli in clones producing T567A and T567D ezrin. Monolayers of P, E, and A cells exhibited comparable microvilli in density and length. In D cultures, above a layer of flat cells, which contain comparable microvilli to P, E, and A cells, some round cells containing numerous and long microvilli were frequently observed. In addition, tufts of microvilli occasionally emerged from flat D cells (right). Bars, 1 μm.

material and cytoskeleton-associated material were compared by immunoblotting, T567A ezrin was highly extracted (Fig. 6 B). After densitometry of the signals, insoluble to soluble ratios were calculated. For exogenous ezrin, as well as endogenous ezrin, the insoluble pool was always less than the soluble pool. However, T567A ezrin was significantly less insoluble than endogenous ezrin, exogenous wt ezrin, or T567D ezrin ($P < 10^{-3}$, ANOVA followed by a Bonferroni *t* test). Therefore, T567A ezrin binds inefficiently to the actin cytoskeleton. Then we examined the distribution of endogenous phosphorylated ERM proteins. Consistently, phosphorylated ERM proteins are enriched in the Triton X-100–insoluble fraction. Taken together, these results indicate that the phosphorylation of the C-ERMAD is required for the association of ERM proteins with the actin cytoskeleton.

Effect of T567A and T567D Ezrin on the Development of Multicellular Epithelial Structures

Organization of the actin cytoskeleton is a crucial point for the establishment and the maintenance of epithelial polarity. Ezrin has been implicated in the development of multicellular epithelial structures (Crepaldi et al., 1997; Gautreau et al., 1999). Therefore, we investigated whether production of T567A ezrin or T567D ezrin affects the morphogenesis of LLC-PK1 cells into suspension cysts and into tubules (Fig. 7).

When isolated LLC-PK1 cells are put in suspension, they aggregate. These aggregates compact in an epithelial cyst with a smooth outline (Wohlwend et al., 1985). By two days, one or several cavities form in these cysts. Cavitation is a hallmark of the development of epithelial polarity. In the hollow cyst, the apical pole is in contact with the medium, whereas the basal pole is in contact with the cavity (Wohlwend et al., 1985). Consistent with the physiology of kidney proximal tubule, formation of this cavity is thought to reflect the vectorial transport of solutes and water from the medium. P, E, and A cells were similarly efficient in the development of hollow suspension cysts. In contrast to these cells, D cells were able to aggregate, but remained in clumps, in which individual round cells could still be distinguished at the periphery. Neither compaction nor cavitation occurred in D cells. This suggests that T567D ezrin impairs the development of epithelial polarity, probably by inducing constant membrane projections.

Consistent with the morphology of kidney proximal tubule, LLC-PK1 cells are able to develop into elongated polarized epithelial structures. Tubulogenesis occurs in a one-week culture in presence of HGF after seeding isolated cells in a three-dimensional collagen type I gel. P cells were able to differentiate into elongated tubules. Overproduction of wt ezrin in E cells potentiated this process and led to long branched tubules, as we previously reported (Crepaldi et al., 1997). In this sensitive assay for ezrin function, production of T567A ezrin impaired tubule formation by affecting clonal growth. By counting cell number, we observed that colonies formed by A cells were always composed of less than five cells, instead of tens of cells for P and E tubules (data not shown). In this assay also, production of T567D ezrin severely impairs epithelial organization of colonies. Colonies of D cells developed into loose aggregates with peripheral cells extending processes in the collagen matrix. D colonies never developed along a well-defined axis. In conclusion, we found that production of T567A ezrin affects tubule development, but

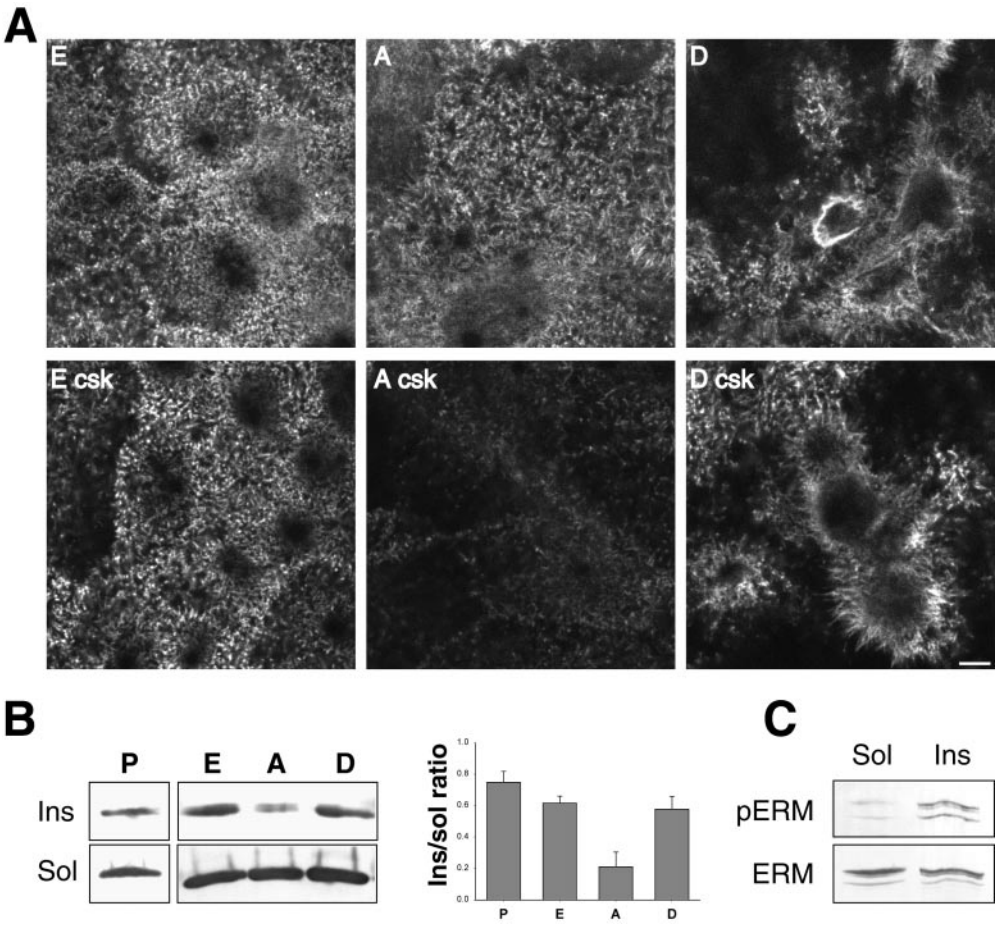

Figure 6. Ezrin association with the actin cytoskeleton requires phosphorylation of T567. (A) Localization of ezrin variants with anti-VSV G antibodies by immunofluorescence and confocal microscopy in E, A, or D cells. Cells were also stained after extraction with a Triton X-100 buffer that preserves cytoskeleton-associated material (csk). A single apical section is shown. Wt, T567A, and T567D ezrin were observed in microvilli. T567D ezrin was also present in the membrane ruffles it induced. After extraction of ezrin-soluble pool, wt and T567D ezrin staining were preserved, whereas T567A ezrin staining was strongly reduced. Bar, 5 μm. (B) Western blot analysis of ezrin cytoskeletal association. Similar fractions of soluble material (Sol), extracted with the Triton X-100 buffer, and insoluble material (Ins), were immunoblotted with anti-ezrin antibodies for P cell extract or with anti-VSV G antibodies for E, A, and D cell extracts. A densitometric analysis was performed and the Ins/Sol ratio was calculated from data obtained from two to four independent experiments with three different A and D clones (mean ± SEM). (C) Soluble and insoluble fractions from LLC-PK1 cells were equalized for their ERM content and immunoblotted with either 297S mAb (pERM) or ERM antibodies. Phosphorylated ERM proteins are enriched in the insoluble fraction.

not suspension cyst morphogenesis, whereas production of T567D ezrin impairs the establishment of epithelial polarity in both assays.

Discussion

In this report, we have examined in vivo the role of ezrin T567 phosphorylation by deriving stable clones producing wt, T567A, and T567D ezrin from the kidney epithelial cell line, LLC-PK1. Since ezrin is present in microvilli both as oligomers and as monomers, it was not known whether the active form of this plasma membrane–actin cytoskeleton linker is monomeric or oligomeric (Berryman et al., 1995; Bretscher, 1999). Our study of T567A and T567D ezrin suggests that the active ezrin linker is a monomer. Given the high conservation of this threonine and of the amino acids forming the interface between the N- and C-ERMAD in ERM from vertebrates, and in homologues from invertebrates, the mechanism of conformational activation by phosphorylation of this conserved threonine from the C-ERMAD probably applies to all members of the ERM family (Pearson et al., 2000).

The Active Plasma Membrane–Actin Cytoskeleton Linker Is a Phosphorylated Monomer

T567A ezrin is poorly associated with microvillar cytoskeleton, as evidenced by the fact that this variant is almost completely extracted by a buffer preserving cytoskeleton-associated material, whereas a significant fraction of wt ezrin is not. This observation confirms in vivo the recent finding that phosphorylation of the homologous threonine 558 in moesin is required for F-actin binding in vitro (Hishiya et al., 1999; Nakamura et al., 1999). Although T567A ezrin is inactive as a cytoskeletal linker, its level of oligomers at the membrane is similar to that of wt ezrin. Thus, the oligomeric species are not sufficient to form active linkers.

The T567D mutation mimics the phosphorylation of this conserved threonine, since both disrupt the N/C-ERMAD interaction in vitro (our results; Matsui et al., 1998). In contrast to T567A ezrin, T567D ezrin is associated with the actin cytoskeleton. Moreover, T567D ezrin is a strongly morphogenic variant. It triggers the formation of wide lamellipodia, extensive membrane ruffles, and microvilli-rich projections, in which T567D ezrin is present.

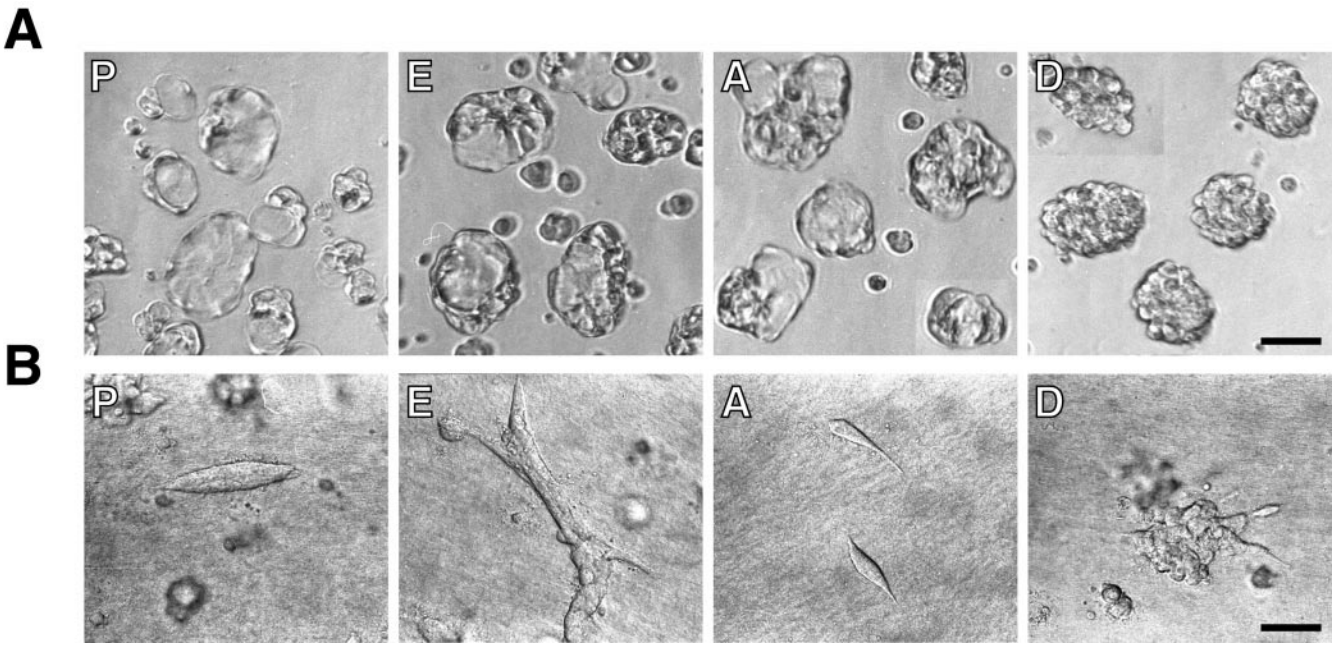

Figure 7. Production of T567A and T567D ezrin affects the development of multicellular epithelial structures. (A) Morphogenesis of suspension cysts examined by phase-contrast optics. Aggregates of LLC-PK1 cells in suspension are able to form hollow epithelial cysts. P, E, and A cells were not affected in this process, whereas D cells formed loose aggregates in which individual cells could still be distinguished at the periphery. (B) Tubulogenesis assay examined by Nomarski optics. In three-dimensional collagen type I, in the presence of HGF, P cells are able to differentiate into multicellular tubules. Production of wt ezrin potentiated growth and branching morphogenesis of tubules. Production of both T567A and T567D ezrin impaired tubulogenesis. A cells exhibited a growth defect, whereas D cells grew in disorganized colonies. Bars, 50 μm.

This finding is consistent with T567D ezrin being an active cytoskeletal linker. By three independent experiments, gel filtration analysis, assay of ezrin homo-oligomers, and ezrin-moesin hetero-oligomers, the level of T567D ezrin oligomers at the membrane was found to be strongly reduced. Thus, the oligomeric species are not necessary to form active linkers. Our study of these two mutant forms of ezrin, which uncouple oligomerization and cytoskeleton binding, provides strong evidence that the active form of this cytoskeletal linker is a phosphorylated monomer. However, it should be pointed out that phosphorylated active ezrin linkers might represent only a minor fraction of membrane monomers, since T567A ezrin exhibits as high a level of monomers at the membrane as wt ezrin.

To confirm this finding made with these ezrin variants, we have analyzed the endogenous phosphorylated ERM proteins. Consistently, we have found that the phosphorylated ERM proteins consist mainly of monomers at the membrane. Moreover, these phosphorylated ERM proteins are Triton X-100–insoluble, suggesting an association with the actin cytoskeleton. Therefore, it is likely that the T567D mutation mimics the phosphorylated state of ezrin in vivo, as well as in vitro, and thus, represents a useful tool to study ezrin function.

Phosphorylation Impairs N/C-ERMAD Interaction of Membrane-bound ERM Proteins

Since T567D ezrin shows a strongly reduced level of membrane oligomers and that phosphorylated ERM proteins are membrane monomers, it is likely that phosphorylation of this conserved threonine in ERM proteins dissociates membrane-bound oligomers into active monomers. It is striking that the phosphorylation-dependent impairment of N/C-ERMAD interaction occurs only on membrane-bound molecules, since the T567D mutation affects neither formation of cytosolic oligomers, nor the correct distribution between cytosol and membrane. Our in vivo analysis suggests the following model of ERM activation. The phosphorylation of a membrane-bound ERM molecule might disrupt intermolecular N/C-ERMAD interaction, thereby dissociating oligomers, and might prevent intramolecular N/C-ERMAD interaction from reforming, thereby exposing its F-actin binding site.

In vitro, phosphorylated moesin binding to F-actin was also found to be strongly dependent on the addition of phosphatidyl-inositol (4,5) bisphosphate or a charged detergent molecule (Nakamura et al., 1999). This result and our in vivo observations suggest that, for the maintenance of the active state, N/C-ERMAD interaction should be abrogated by both phosphorylation of the C-ERMAD and lipid binding to the N-ERMAD. This double regulation of ERM proteins is highly significant for these plasma membrane–actin cytoskeleton linkers. This double regulation might also explain that, despite the strong morphogenic effects of T567D ezrin, no more T567D ezrin than wt ezrin is Triton X-100–insoluble. This suggests that an activation factor other than phosphorylation is limiting the amount of cytoskeleton-bound ezrin. Since inactivation of ERM linkers occurs presumably through dephosphorylation of

this conserved threonine (Fukata et al., 1998; Hishiya et al., 1999), T567D ezrin might be morphogenic, because, in contrast to wt ezrin, this variant cannot be dephosphorylated. The T567D mutation presumably locks the membrane pool of T567D ezrin in its active conformation.

What Is the Role of ERM Oligomers?

Since the dormant cytosolic form of ERM proteins is monomeric and the active plasma membrane–cytoskeleton linker is also monomeric, the role of oligomers in the activation pathway is rather intriguing. Formation of oligomers requires the conformational opening of monomers and the condensation of two, or more, opened monomers. The molecular components of the machinery required for oligomer formation are unknown. Membrane binding sites are cryptic in the dormant monomer, since a deletion of the C-ERMAD is sufficient to allow membrane recruitment of Δ29 ezrin. This truncated molecule is monomeric, indicating that oligomerization is not required, per se, for membrane recruitment. Also intriguing is the observation that Δ29 ezrin, despite having an exposed N-ERMAD, does not form oligomers, or at least dimers. One possible explanation is that the machinery for oligomer formation is only present in the cytosol, and is not accessible to the membrane-bound Δ29 ezrin. Since ezrin oligomers exist in cytosolic and membrane pools, asymmetric oligomers, having an exposed N-ERMAD (Bretscher, 1999), might be in equilibrium between the cytosol and the membrane.

Phosphorylation of Ezrin on T567 Transduces Morphogenic and Growth Signals

ERM proteins are known to be essential for actin-rich membrane projections (Takeuchi et al., 1994; Crepaldi et al., 1997; Lamb et al., 1997; Bretscher, 1999). Various stimuli that trigger the formation of these membrane structures induce ERM phosphorylation on this threonine residue (Nakamura et al., 1995; Matsui et al., 1999; Yonemura et al., 1999). Moreover, we showed that the production of T567D ezrin in LLC-PK1 cells induces a variety of actin-rich membrane projections, wide lamellipodia, membrane ruffling, and projections covered with microvilli, appearing as tufts of microvilli. Therefore, phosphorylation of this threonine residue on membrane ERM proteins appears to be critical for the generation of actin-rich membrane projections.

However, it is surprising that the mere production of an active linker tethering actin cytoskeleton to the plasma membrane induces such structures. Indeed, these membrane projections require several other coordinated processes, such as actin polymerization and cross-linking of actin filaments. Thus, T567D ezrin, in addition to being an active linker, induces a complete program for the formation of lamellipodia and ruffles. This is evidence of signaling events from active ezrin to the machineries controlling actin polymerization and cross-linking. These constitutive signaling events from T567D ezrin to actin dynamics and the consequent formation of membrane projections might explain why LLC-PK1 cells producing this ezrin variant fail to achieve epithelial polarity, as seen in suspension cyst and tubulogenesis assays.

In contrast, production of the inactive linker T567A ezrin did not affect epithelial polarity, as evidenced by the development of suspension cysts. In LLC-PK1 cells, production of the inactive T567A ezrin does not impair the formation of epithelial microvilli, whereas in transiently transfected COS7 cells, T558A moesin was reported to inhibit the RhoA-dependent formation of microvilli-like structures (Oshiro et al., 1998). However, T567A ezrin was found to be dominant negative in a tubulogenesis assay.

Differentiation of tubules in three-dimensional collagen matrix in the presence of HGF is a cellular assay critically dependent on ezrin function. Some phenotypes associated with expression of wt or mutant ezrin cDNAs are detected uniquely in these differentiation conditions. As reported previously, ezrin overproduction potentiates elongation and branching of tubules (Crepaldi et al., 1997). Production of Y353F ezrin specifically triggered apoptosis in this tubulogenesis assay (Gautreau et al., 1999). Here, production of T567A ezrin affected growth of LLC-PK1 cells in these conditions. One possible mechanism for this dominant negative effect is that overproduced inactive T567A ezrin is membrane-recruited instead of endogenous ezrin, and thereby impairs its function. In this tubulogenesis assay, phosphorylation of ezrin T567, and activation of its linker function, are needed for proliferation signaling. In 3T3 cells, T567A ezrin was also found to inhibit Ras- and Rho-dependent cellular transformation (Tran Quang, C., A. Gautreau, M. Arpin, and R. Treisman, manuscript submitted for publication). How ezrin signals proliferation is presently not known, but this signaling ability of ezrin relates to the activation of its linker function by phosphorylation of T567.

In the present study, we described the role of ezrin phosphorylation on T567 in vivo. This phosphorylation event regulates a membrane-specific transition of this actin cytoskeleton linker from inactive oligomers to active monomers. This unanticipated step of ezrin activation is critical for cell shape and growth during epithelial differentiation.

We thank Dr. P. Mangeat and Dr. S. Tsukita for providing generously antibodies; L. Del Maestro for technical assistance; Lucien Cabanié for his help in chromatography; M. Grasset for her help in scanning EM; Dr. M. Beckerle, Dr. P. Mangeat, and Dr. P. Poullet for helpful comments on the manuscript.

This work was supported by a grant from the Association pour la Recherche sur le Cancer (ARC 9663) and by a fellowship from the Ministère de l'Education Nationale, de la Recherche et de la Technologie to A. Gautreau.

Submitted: 3 March 2000
Revised: 15 May 2000
Accepted: 5 June 2000

References

Algrain, M., O. Turunen, A. Vaheri, D. Louvard, and M. Arpin. 1993. Ezrin contains cytoskeleton and membrane binding domains accounting for its proposed role as a membrane–cytoskeletal linker. *J. Cell Biol.* 120:129–139.

Andréoli, C., M. Martin, R. Le Borgne, H. Reggio, and P. Mangeat. 1994. Ezrin has properties to self-associate at the plasma membrane. *J. Cell Sci.* 107: 2509–2521.

Berryman, M., Z. Franck, and A. Bretscher. 1993. Ezrin is concentrated in the apical microvilli of a wide variety of epithelial cells whereas moesin is found primarily in endothelial cells. *J. Cell Sci.* 105:1025–1043.

Berryman, M., R. Gary, and A. Bretscher. 1995. Ezrin oligomers are major cytoskeletal components of placental microvilli: a proposal for their involvement in cortical morphogenesis. *J. Cell Biol.* 131:1231–1242.

Bretscher, A. 1999. Regulation of cortical structure by the ezrin-radixin-moesin protein family. *Curr. Opin. Cell Biol.* 11:109–116.

Bretscher, A., R. Gary, and M. Berryman. 1995. Soluble ezrin purified from placenta exists as stable monomers and elongated dimers with masked C-terminal ezrin-radixin-moesin association domains. *Biochemistry*. 34:16830–16837.

Chen, J., R.B. Doctor, and L.J. Mandel. 1994. Cytoskeletal dissociation of ezrin during renal anoxia: role in microvillar injury. *Am. J. Physiol.* 267:C784–C795.

Crepaldi, T., A. Gautreau, P.M. Comoglio, D. Louvard, and M. Arpin. 1997. Ezrin is an effector of hepatocyte growth factor-mediated migration and morphogenesis in epithelial cells. *J. Cell Biol.* 138:423–434.

Fazioli, F., W.T. Wong, S.J. Ullrich, K. Sakaguchi, E. Appella, and P.P. Di Fiore. 1993. The ezrin-like family of tyrosine kinase substrates: receptor-specific pattern of tyrosine phosphorylation and relationship to malignant transformation. *Oncogene.* 8:1335–1345.

Fukata, Y., K. Kimura, N. Oshiro, H. Saya, Y. Matsuura, and K. Kaibuchi. 1998. Association of the myosin binding subunit of myosin phosphatase and moesin: dual regulation of moesin phosphorylation by rho-associated kinase and myosin phosphatase. *J. Cell Biol.* 141:409–418.

Gary, R., and A. Bretscher. 1993. Heterotypic and homotypic associations between ezrin and moesin, two putative membrane–cytoskeletal linking proteins. *Proc. Natl. Acad. Sci. USA*. 90:10846–10850.

Gary, R., and A. Bretscher. 1995. Ezrin self-association involves binding of an N-terminal domain to a normally masked C-terminal domain that includes the F-actin binding site. *Mol. Biol. Cell.* 6:1061–1075.

Gautreau, A., P. Poullet, D. Louvard, and M. Arpin. 1999. Ezrin, a plasma membrane–microfilament linker, signals cell survival through the phosphatidylinositol 3-kinase/Akt pathway. *Proc. Natl. Acad. Sci. USA*. 96:7300–7305.

Gould, K.L., A. Bretscher, F.S. Esch, and T. Hunter. 1989. cDNA cloning and sequencing of the protein-tyrosine kinase substrate, ezrin, reveals homology to band 4.1. *EMBO (Eur. Mol. Biol. Organ.) J.* 8:4133–4142.

Hayashi, K., S. Yonemura, T. Matsui, S. Tsukita, and S. Tsukita. 1999. Immunofluorescence detection of ezrin/radixin/moesin (ERM) proteins with their carboxyl-terminal threonine phosphorylated in cultured cells and tissues: application of a novel fixation protocol using trichloroacetic acid (TCA) as a fixative. *J. Cell Sci.* 112:1149–1158.

Hishiya, A., M. Ohnishi, S. Tamura, and F. Nakamura. 1999. Protein phosphatase 2C inactivates F-actin binding of human platelet moesin. *J. Biol. Chem*. 274:26705–26712.

Huang, L.Q., T.Y.W. Wong, R.C.C. Lin, and H. Furthmayr. 1999. Replacement of threonine 558, a critical site of phosphorylation of moesin in vivo, with aspartate activates F-actin binding of moesin: regulation by conformational change. *J. Biol. Chem*. 274:12803–12810.

Kondo, T., K. Takeuchi, Y. Doi, S. Yonemura, S. Nagata, and S. Tsukita. 1998. ERM (ezrin/radixin/moesin)-based molecular mechanism of microvillar breakdown at an early stage of apoptosis. *J. Cell Biol.* 139:749–758.

Krieg, J., and T. Hunter. 1992. Identification of the two major epidermal growth factor-induced tyrosine phosphorylation sites in the microvillar core protein ezrin. *J. Biol. Chem*. 267:19258–19265.

Lamb, R.F., B.W. Ozanne, C. Roy, L. McGarry, C. Stipp, P. Mangeat, and D.G. Jay. 1997. Essential functions of ezrin in maintenance of cell shape and lamellipodial extension in normal and transformed fibroblasts. *Curr. Biol.* 7:682–688.

Magendantz, M., M.D. Henry, A. Lander, and F. Solomon. 1995. Interdomain interactions of radixin in vitro. *J. Biol. Chem*. 270:25324–25327.

Matsui, T., M. Maeda, Y. Doi, S. Yonemura, M. Amano, K. Kaibuchi, and S. Tsukita. 1998. Rho-kinase phosphorylates COOH-terminal threonines of ezrin/radixin/moesin (ERM) proteins and regulates their head-to-tail association. *J. Cell Biol.* 140:647–657.

Matsui, T., S. Yonemura, S. Tsukita, and S. Tsukita. 1999. Activation of ERM proteins in vivo involves phosphatidylinositol 4-phosphate 5-kinase and not ROCK kinases. *Curr. Biol.* 9:1259–1262.

Nakamura, F., M.R. Amieva, and H. Furthmayr. 1995. Phosphorylation of threonine 558 in the carboxyl-terminal actin-binding domain of moesin by thrombin activation of human platelets. *J. Biol. Chem*. 270:31377–31385.

Nakamura, F., M.R. Amieva, C. Hirota, Y. Mizuno, and H. Furthmayr. 1996. Phosphorylation of 558T of moesin detected by site-specific antibodies in RAW264.7 macrophages. *Biochem. Biophys. Res. Comm*. 226:650–656.

Nakamura, F., L. Huang, K. Pestonjamasp, E.J. Luna, and H. Furthmayr. 1999. Regulation of F-actin binding to platelet moesin in vitro by both phosphorylation of threonine 558 and polyphosphatidylinositides. *Mol. Biol. Cell.* 10: 2669–2685.

Oshiro, N., Y. Fukata, and K. Kaibuchi. 1998. Phosphorylation of moesin by rho-associated kinase (Rho-kinase) plays a crucial role in the formation of microvilli-like structures. *J. Biol. Chem*. 273:34663–34666.

Pearson, M.A., D. Reczek, A. Bretscher, and P.A. Karplus. 2000. Structure of the ERM protein moesin reveals the FERM domain fold masked by an extended actin binding tail domain. *Cell.* 101:259–270.

Pietromonaco, S.F., P.C. Simons, A. Alman, and L. Elias. 1998. Protein kinase C-theta phosphorylation of moesin in the actin-binding sequence. *J. Biol. Chem*. 273:7594–7603.

Reczek, D., and A. Bretscher. 1998. The carboxy-terminal region of EBP50 binds to a site in the amino-terminal domain of ezrin that is masked in the dormant molecule. *J. Biol. Chem*. 273:18452–18458.

Reczek, D., M. Berryman, and A. Bretscher. 1997. Identification of EBP50: A PDZ-containing phosphoprotein that associates with members of the ezrin-radixin-moesin family. *J. Cell Biol.* 139:169–179.

Shaw, R.J., M. Henry, F. Solomon, and T. Jacks. 1998. RhoA-dependent phosphorylation and relocalization of ERM proteins into apical membrane/actin protrusions in fibroblasts. *Mol. Biol. Cell.* 9:403–419.

Simons, P.C., S.F. Pietromonaco, D. Reczek, A. Bretscher, and L. Elias. 1998. C-terminal threonine phosphorylation activates ERM proteins to link the cell's cortical lipid bilayer to the cytoskeleton. *Biochem. Biophys. Res. Comm*. 253:561–565.

Takahashi, K., T. Sasaki, A. Mammoto, K. Takaishi, T. Kameyama, S. Tsukita, and Y. Takai. 1997. Direct interaction of the Rho GDP dissociation inhibitor with ezrin/radixin/moesin initiates the activation of the Rho small G protein. *J. Biol. Chem*. 272:23371–23375.

Takeuchi, K., N. Sato, H. Kasahara, N. Funayama, A. Nagafuchi, S. Yonemura, and S. Tsukita. 1994. Perturbation of cell adhesion and microvilli formation by antisense oligonucleotides to ERM family members. *J. Cell Biol.* 125: 1371–1384.

Turunen, O., T. Wahlstrom, and A. Vaheri. 1994. Ezrin has a COOH-terminal actin-binding site that is conserved in the ezrin protein family. *J. Cell Biol.* 126:1445–1453.

Wohlwend, A., R. Montesano, J.D. Vassalli, and L. Orci. 1985. LLC-PK1 cysts: a model for the study of epithelial polarity. *J. Cell. Physiol.* 125:533–539.

Yonemura, S., S. Tsukita, and S. Tsukita. 1999. Direct involvement of ezrin/radixin/moesin (ERM)-binding membrane proteins in the organization of microvilli in collaboration with activated ERM proteins. *J. Cell Biol.* 145:1497–1509.